

AN APPROACH STUDY TO SELECTIVE LASER SINTERING (SLS) OF PRE-COATED SANDS FOR SHELL-MOULDING

G. Dini Department of Mechanical, Nuclear and
M. Lanzetta Production Engineering
M. Santochi University of Pisa
G. Tantussi

A. Franco Department of Energetics, University of Pisa

KEY WORDS: Selective Laser Sintering, Shell-Moulding, Heat Transfer

ABSTRACT: The Selective Laser Sintering of pre-coated sands is a promising Rapid Prototyping technique for the construction of sand shells for foundry. In this article, the definition of mathematical simulation concepts and a detailed experimental analysis, performed both with conventional and unconventional techniques, is proposed. In particular, two methods to calculate the temperature distribution within the sand bed and the depth of the heat-affected zone are studied. The results obtained with the experimental methodology and those coming from previous experimental analyses have been used to validate the described mathematical models, that represent a first step for the process comprehension, control and optimisation. Two kinds of pre-coated sands, widely used in shell-moulding, have been considered: zirconia and silica. The guidelines for future simulation refinements are also given.

1. INTRODUCTION

Selective Laser Sintering (SLS) is a process to create solid objects, layer by layer, from

plastic, metal, ceramic powders or pre-coated sands that are «sintered» using laser energy. The basic concept, common to all rapid-prototyping techniques, is that any complex shape can be obtained with the superposition of small thickness layers. The inherent material versatility of SLS technology allows a broad range of advanced rapid prototyping and manufacturing applications to be addressed [1]. In Figure 1. a SLS application for foundry shell construction is schematically described and compared with the traditional process.

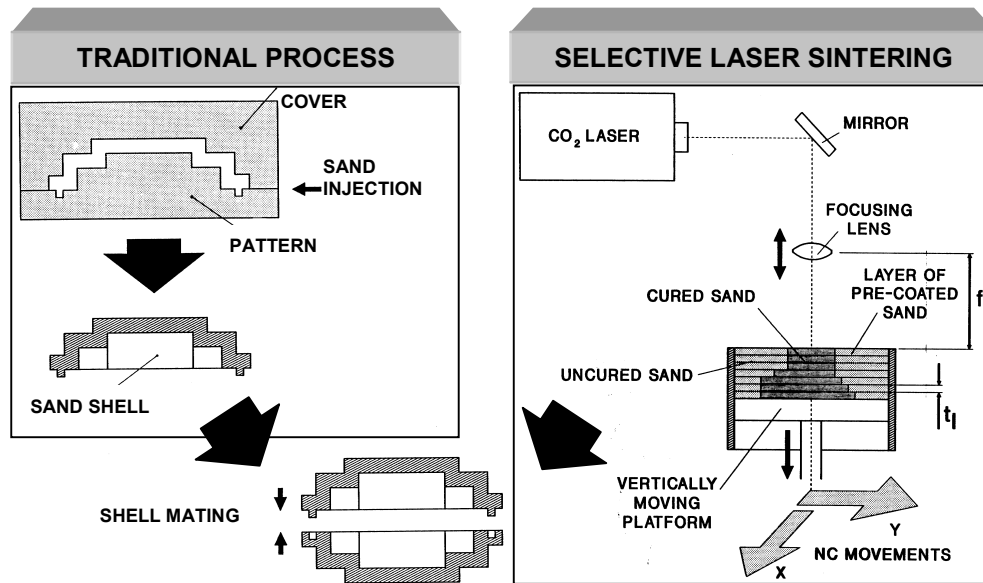


Figure 1. - Comparison between the traditional method and SLS to obtain foundry shells

To achieve parts with acceptable geometry and strength, the following problems should be considered:

- to obtain a reliable adhesion between layers;
- to generate flat surfaces without distortions;
- to obtain a suitable resolution.

Several studies on SLS have been carried out in the last years, but the heat conduction and energy release mechanism, that determines the grain agglomeration, has not yet been completely investigated both on the experimental and theoretical point of view. Only recently, strategies for the simulation of the SLS process related to metallic powders have been developed both in [2] - where Polymer Coated Silicon Carbide Powders as the base material is considered - and in [3-4] - where Polycarbonate is used - but available methods do not provide sufficient details for their application.

In [5], the authors described an experimental facility to investigate the SLS process of pre-coated sands for shell-moulding. The present work continues this analysis, considering the sand thermo-physical properties and the measurement of the real input energy. In addition, two possible mathematical models of the SLS process are proposed and tested.

2. THE PROCESS PARAMETERS

The main technological parameters to control the SLS process are:

- the pre-coated sand and its thermo-physical properties, such as density ρ , specific heat c_p , thermal conductivity k , resin polymerisation temperature range ΔT_p , sand glass-transition temperature T_g , sand energy absorption a , reflection r and transmission τ coefficients, and other properties, such as granulometry and average grain dimension;
- the scan spacing;
- the laser beam power P ;
- the laser spot diameter \varnothing ;
- the scan speed V .

The four sand types under study, belonging to two categories (Table I), are commonly used in shell-moulding as they have a good compatibility to the fused metallic material.

Table I - Commercial sand properties

| Sand type | Commercial name | Composition | Density [kg/m ³] | Resin weight [%] | Granulometry [DIN 1171] | Average grain size [mm] |
|-----------|-----------------|------------------------------------|------------------------------|------------------|-------------------------|-------------------------|
| zirconia | Zircon | ZrO ₂ 99.6 % | 2810 | 2.5 | 61 | 0.19 |
| silica | DB 40 | Si ₂ O ₃ 95% | 1600 | 3.4 | 79 | 0.14 |
| silica | LHN 50/70 | “ | 1560 | 4.0 | 57 | 0.20 |
| silica | E 45 | “ | 1555 | 3.8 | 108 | 0.10 |

The last three process parameters determine the thermal radiant power density, that depends directly on the laser power and inversely on the spot diameter and the scan speed; this latter has a direct impact on productivity.

On the other hand, the shell mechanical resistance is influenced by the depth p of the heat-affected zone (strictly related to the layer thickness t_l of Figure 1.) and by the temperature history determined by the laser radiation, and finally by the process parameters.

In this particular SLS application, the laser beam raises the sand temperature allowing the agglomeration of grains, without local burning. Under the thermal viewpoint, the phenomenon can be schematically described as follows: the energy absorbed by the sand leads the resin into a glass-like state so that grains coalesce into a solid (Figure 2.). The temperature necessary to reach this condition seems lower than the one at which resin polymerisation occurs [5].

It appears that SLS is basically a heat transmission phenomenon in which the input energy, the laser radiation, generates in the sand bed a mixed conduction and convection heat transfer. The grain agglomeration strongly depends on the energy absorbed by the sand bed and on the energy required for the resin polymerisation, as well as on the chemical energy release during the heating process.

To set the optimum thermal radiant power density in order to maximise the productivity and to find a suitable compromise between the quality and the mechanical resistance of shells, a suitable combination of the three parameters should be determined.

A quantitative understanding of the temperature gradient, and of the depth of the heat-affected zone and their dependence on the input parameters allows the generation of quality forms and a thermal control of the working area.

3. THE SLS PROCESS MODELISATION

SLS is a very dynamic process, hence its mathematical description involves the solution of the *unsteady* heat conduction equation. The model should reproduce the thermal history within the sand bed after the radiation incidence starts. As already mentioned, simplified modelisations of the SLS process can be found in the literature, but they are generally related to metallic powder operating at higher temperature range [2-4].

In this paper the application of a heat conduction scheme to the SLS of pre-coated sands and a refinement of the existing models is proposed, having in mind to maintain a simple approach. Moreover, differently with respect to other studies, an attempt to provide a general method that can be simply tested by other researchers with the same or with a different base material has been made. The material (a pre-coated sand) is considered as homogeneous from the thermal point of view and its thermo-physical properties do not change with temperature. With these hypotheses, the chemical aspects related to the energy absorbed and released during heating are considered.

In our model, as in the majority of those proposed in the literature, the governing equation is the unsteady heat conduction equation. The resulting output data are:

- the temperature distribution and the maximum value on the surface T_{max} ;
- the depth p and the width of the heat-affected zone considered as the penetration of the isothermal front corresponding to the resin glass-transition temperature.

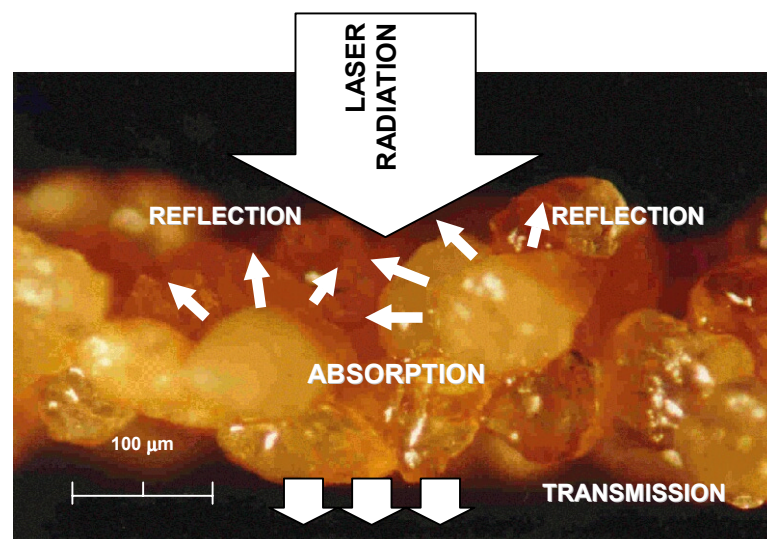


Figure 2. - Energy flow in the SLS general process

This last hypothesis is a direct consequence of the experimental investigation in [5], where it was observed that the sand grain agglomeration occurs before reaching the resin polymerisation temperature. This kind of model, though simplified, could be a theoretical instrument for preliminary evaluation of the operative parameters in order to avoid unsatisfactory technological results such as high surface temperatures, high polymerisation thickness or burnt sand. When the laser spot hits the sand bed, the surface interaction with the radiant energy can be described by the coefficients representing the fraction of absorbed a , reflected r , and transmitted energy τ (Figure 2.); of course,

$$r + a + \tau = 1 \quad (1)$$

The three coefficients depend on the sand used, on the resin, and on the radiation itself, but they are very difficult to obtain from the literature. For the pre-coated sands used in shell-moulding, the absorptivity coefficient a is sensibly higher than 0.9 and the reflectivity is lower than 0.01 [6].

As mentioned before, the penetration of the glass-transition temperature front into the sand bed determines the depth and width of the heat-affected zone. However this thermal problem, even if conceptually simple, has not a simple solution for the following reasons:

- the intrinsic complexity of the phenomenon and of its mathematical scheme (three-dimensional thermal conduction with convective surface heat dissipation);
- the difficulties in the characterisation of the sands from a thermo-physical point of view (thermal conductivity, specific heat capacity and thermal diffusivity);
- the difficulties in a correct modelisation of the pre-coated sands from a chemical point of view (polymerisation temperature, energy released during the polymerisation process caused by the breakage of chemical links, etc.).

Moreover it would be necessary to consider the following aspects that are usually neglected in the modelisation:

- the influence of mechanical phenomena, like the sand agglomeration caused by friction and by special thermo-hygrometric conditions;
- the effects of the non-homogeneous material;
- the changes of the pre-coated sand thermo-physical properties with the temperature.

3.1 The analytical solution of the 1D heat conduction equation

A first method to model the SLS process is represented by the one-dimensional heat conduction transfer equation. In this scheme, the heat transfer in a plane perpendicular to the laser radiation incidence is neglected and the heat transfer by conduction is studied only in the direction of the laser beam axis z ; the material is considered as homogeneous.

The phenomenon is governed by the general one-dimensional heat conduction equation in unsteady conditions:

$$\frac{\partial T}{\partial t} = \frac{k}{\rho \cdot c_p} \cdot \frac{\partial^2 T}{\partial z^2} \quad (2)$$

with the following boundary conditions:

$$k \frac{\partial T}{\partial z} \Big|_{z=0} = \dot{q}'' = a \cdot \dot{q} - h(T - T_\infty) \quad t \leq t^* \quad k \frac{\partial T}{\partial z} \Big|_{z=0} = -h(T - T_\infty) \quad t > t^*$$

where h is the convective heat transfer coefficient between surface and surrounding air (that can be conventionally assumed equal to $10 \text{ W/m}^2\text{K}$ for natural convection), \dot{q} is the specific thermal power of laser radiation (in W/m^2) expressed by $P/(\varnothing \times s)$, being s the space hit by laser in the unit of time, T_∞ is the environmental temperature, and t^* is the radiation incidence duration.

A closed solution of the thermal conduction problem expressed by (2) can be obtained by supposing that the thermal influenced zone, exposed since the time $t = 0$ to a heat flux \dot{q}'' , is small with respect to the working area. Until $t = t^*$, the temperature history during the radiation incidence can be expressed as follows:

$$T(z, t) = T_i + 2 \frac{\dot{q}''}{k} \cdot \left(\frac{\alpha t}{\pi} \right)^{1/2} \exp\left(-\frac{z^2}{4\alpha t}\right) - \frac{\dot{q}''}{k} \cdot z \cdot \text{erfc}\left[\frac{z}{2(\alpha t)^{1/2}}\right] \quad (3)$$

where $\alpha = k / (\rho c_p)$ is the sand thermal diffusivity, T_i the initial temperature of the sand bed and erfc is the complementary error function [7].

For $t > t^*$:

$$\frac{T(z, t) - T_\infty}{T_f - T_\infty} = \text{erf}\left[\frac{z}{2(\alpha t)^{1/2}}\right] + \exp\left(\frac{hz}{k} + \frac{h^2 \alpha t}{k^2}\right) \text{erfc}\left[\frac{z}{2(\alpha t)^{1/2}} + \frac{h}{k}(\alpha t)^{1/2}\right] \quad (4)$$

where T_f is the surface temperature at the end of the heating process and erf is the error function [7].

To improve the one-dimensional schematisation, it is possible to consider that the sand temperature T_i in the equation (3) is the environmental temperature at the initial step only. In the next steps, it is necessary to take into account the effects connected with the laser incidence in the adjacent region.

In order to consider the two-dimensional effects of the thermal heat conduction, a different schematisation of the laser incidence is then used: the well known «moving heat source» (that allows the simulation of arc welding and surface hardening as well) [7]. In this way it is possible to evaluate the temperature field deformation, when the heat source moves through the conductive medium, by adjusting the initial condition for the application of (3) and by evaluating the influence of the laser radiation in a plane perpendicular to the z axis to estimate the width of the heat-affected zone also. With a heat source moving in the x direction, the temperature history in the (x, y) plane can be expressed by:

$$T(x, y) = T_\infty + \frac{\dot{q}' \rho c_p}{(4\pi V \alpha x)} \exp\left(-\frac{Vy^2}{4\alpha x}\right) \quad (5)$$

where $\dot{q}' = P/p$ is the *linear* density of the heat flux expressed in W/m . The depth of the

heat-affected zone p is adjusted in order to provide the same value of the maximum temperature obtained with the equation (3).

3.2 The numerical solution of the 3D heat conduction equation

To simulate in a more complete way the heat transmission related to SLS, it is necessary to consider the three-dimensional heat conduction problem in a sufficiently large object, made of homogeneous material, with the moving heat source boundary conditions [8].

This problem is not easy to solve and the hypothesis of a small thermal influenced zone with respect to the working area cannot be removed.

An alternative method consists in applying to a finite sand bed volume the three-dimensional time-dependent conduction problem expressed in the classical form as:

$$\rho c_p \frac{\partial T}{\partial t} = \frac{\partial}{\partial x} \left(k \frac{\partial T}{\partial x} \right) + \frac{\partial}{\partial y} \left(k \frac{\partial T}{\partial y} \right) + \frac{\partial}{\partial z} \left(k \frac{\partial T}{\partial z} \right) + q_v \quad (6)$$

that is valid for isotropic, heterogeneous media, where $q_v(x, y, z, t)$ is the heat generated per unit of time and space, to be defined from the boundary conditions of the equation (2), and k , ρ and c_p depend on space and time, for their dependence on the temperature. In this case the radiation is considered as one-dimensional but the conduction within the sand is three-dimensional.

Obviously an analytical solution of the equation (6) with this hypothesis is not currently available but a solution based on numerical methods is possible, through the discretisation of the spatial - by means of cubic cells - and of the temporal domains. The solution is a function $T(x, y, z, t)$ and a finite domain is considered.

An attempt to solve the three-dimensional problem represented by the equation (6), transformed in the form of a transport equation for the static enthalpy, has been made in this work by means of a commercial computational code, FLUENT, with the SIMPLER algorithm [9]. With this particular code, the sand porosity can also be considered, by activating the porous media modelling option.

The program flexibility allows a complete schematisation of the thermal phenomenon, including the influence produced by the increase of temperature in the proximity of the radiation incidence point, and consequently it allows a correct definition of the heat-affected zone width, that cannot be considered directly in the one-dimensional model.

While the analytical solution of the equation (2) by means of the equations from (3) to (5) permits to investigate the influence of the laser power, the scan speed and the spot diameter, with the three-dimensional schematisation it is also possible to investigate the influence of the scan spacing. But the modelisation of the moving heat source, representing the laser beam and its transformation in a time-dependent volumetric heat source, is a very critical aspect, with the available options of the numerical code.

4. EXPERIMENTAL TESTS

An experimental investigation was performed to define the real mechanism causing the

sand agglomeration, to calculate the sand thermo-physical properties and to determine the actual heat amount absorbed by the sand bed. The obtained data and those coming from previous experimental analysis [5] have been used to validate the described models.

The following analyses have been carried out:

- a) analysis on the SLS process through general tests;
 - b) collection of the necessary parameters through the characterisation of the used sands;
 - c) determination of the energy transmission coefficients.
- a) In order to test the models and their possibility to simulate the real layer thickness and the temperature values, the experimental facility described in [5] has been used. This analysis permitted to determine the influence of the most important process parameters, described in 2. on some aspects of the process, such as the width and the depth of the heat-affected zone and the temperature distribution. This last variable has been measured through an IR TV camera, whose error assessment is critical, especially at high scan speed.

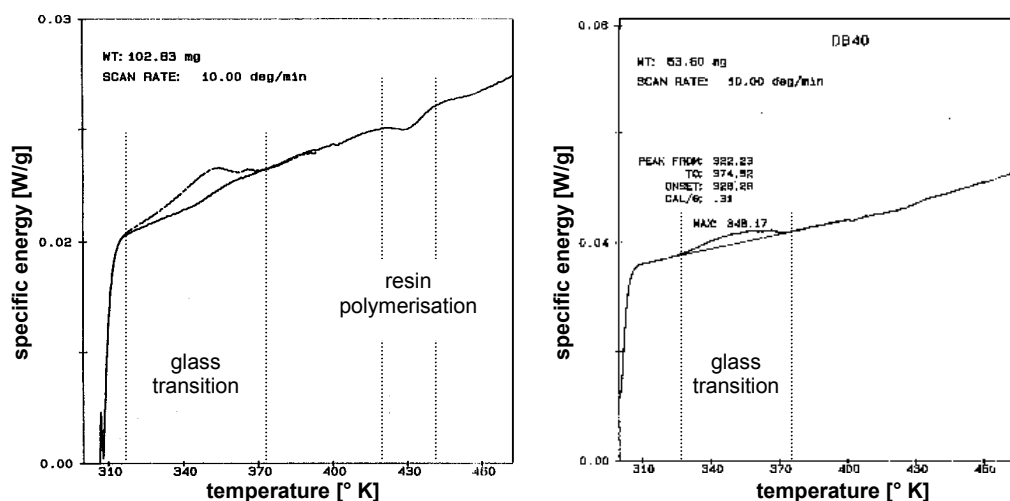


Figure 3. - DSC analysis - a. Zirconia - b. Silica DB40

- b) During tests, two different sands have been used, Zircon and DB40, as the three silica sands in Table I have similar thermo-physical properties. The following thermo-physical sand properties have been determined in laboratory tests: the specific heat, the thermal conductivity and the energy absorption during the heating process.

The specific heat was measured by means of calorimetric Peltier analysis using a Calvet calorimeter. It is calculated by comparison with the specific heat of water, by comparing the heat transferred in a definite time to a metallic cell by the two substances, contained inside analogous cells, starting from the same initial temperature.

The thermal conductivity k of the pre-coated sands, once that the specific heat c_p was determined, has been extrapolated from the same analysis, starting from the time

necessary to cool the sand contained inside the metallic cell and from the knowledge of the reference substance, the water.

To investigate in detail the nature of the agglomeration process, both the resin and the sand were exposed to Differential Scanning Calorimetric (DSC) analysis [10], that permitted also to evaluate the energy released during the heating process. In Figure 3.a. and b. the results of the two investigations relatively to zirconia and silica sand are shown. The analysis confirms the validity of one of the basic hypotheses of our modelisation, scarcely considered in the literature about foundry: the most important transformation evidenced by the analysis takes place at a temperature of about 75-80° C (that can be assumed as the glass-transition temperature T_g) and it is lower than the polymerisation temperature of the phenolic resin, about 155° C.

The DSC analysis evidences a small heat release, three or four orders of magnitude lower than the laser beam radiant energy, near the temperature corresponding to the glass-transition, characterised by a decreasing slope of the curves (Figure 3.).

Table II - Sand properties determined in laboratory tests

| Sand | c_p [J/kg K] | k [W/m K] | $\alpha=k / (\rho c_p)$ [m ² /s] | T_g [° C] |
|--------|-------------------|--------------|--|----------------|
| Zircon | 580.7 | 0.74 | $4.53 \cdot 10^{-7}$ | 78 |
| DB40 | 774.4 | 0.53 | $4.27 \cdot 10^{-7}$ | 75 |

In Table II the main thermo-calorimetric results of the investigated sands are shown. In particular the values of the thermal conductivity k are similar to those provided by other researchers [6]. No reference values are available for the other thermo-physical properties.

c) A specific analysis concerning the energy distribution within the sand, to obtain the terms a and τ of the equation (1), has been carried on too. A schematisation of the experimental analysis is shown in Figure 4. The values of the absorption and transmission coefficients, have been obtained with the following method:

- the nominal laser beam power is indicated on a power meter installed on the laser;
- the effective laser beam power on the sand bed has been measured with a power gauge, based on the thermal balance between incising and dispersed heat;
- the transmitted energy has been measured with the same power gauge, after its positioning under sand layers of different thickness (detail of Figure 4.);
- the reflected energy r is lower than 1%.

The sand absorption coefficient a has been obtained with equation (1). Considering that only a small amount of the energy is reflected and not more than 2-4% is transmitted at higher depth than 0.2 mm, 95% of the radiant energy is adsorbed by the sand, as expected [6]. Finally, for the calculation:

$$a = 0.95-0.97 \quad \tau = 0.02-0.04 \quad r = 0.01$$

5. DISCUSSION OF RESULTS AND CONCLUSIONS

The mathematical models described in 3.1 and 3.2 have been assessed making use of the data provided by the experimental analyses: those provided in [5], concerning the maximum surface temperature $T(z = 0)$ and the depth of the heat-affected zone p , and by using the sand thermo-physical properties acquired in this work. The results, for some combinations of the input parameters, are shown in Tables III and IV for Zircon and DB40 respectively.

From Tables III and IV it can be observed that in most cases both the models tend to *overestimate* the sand bed temperature and to *underestimate* the agglomeration depth. The experimental measurement of the sand layer depth p , made manually with a microscope, is critical (Figure 2.) and the results can be overestimated about one grain size (Table II). On the other hand, the maximum surface temperature T_{\max} can be underestimated with the used technique. This problem is dealt with in the literature [11].

The best results can be obtained for scan speed higher than 1000 mm/min, in particular for the analytical model. It is necessary to point out that the speed values of this order of magnitude are those interesting for industrial applications.

It is also possible to underline that better results have been obtained simulating the silica sand rather than the zirconia sand. The three-dimensional numerical analysis provides good results for a laser spot diameter of 1.2 mm and generally overestimates the surface temperature. This effect is probably due to numerical convergence on the boundary cells caused by their small dimension in relation to the high specific input power.

The difference between experiments and simulation for both the heat-affected zone depth p and the temperature T_{\max} may be caused by an incorrect experimental estimation of the laser beam input power \dot{q} , as well as by some of the simplified basic model hypotheses, related to the following aspects:

1. The material has been considered isotropic and its thermal conductivity has been considered not depending on the direction, but the sand grain geometry could determine preferential directions for the heat conduction.
2. The sand thermo-physical properties, mainly the thermal conductivity and the specific heat, could vary according to the increase of temperature and to the resin agglomeration state.
3. Only the thermal diffusion has been considered to reach the glass-transition temperature and consequently for the grain agglomeration. Local phenomena related to chemical reactions could be important too.

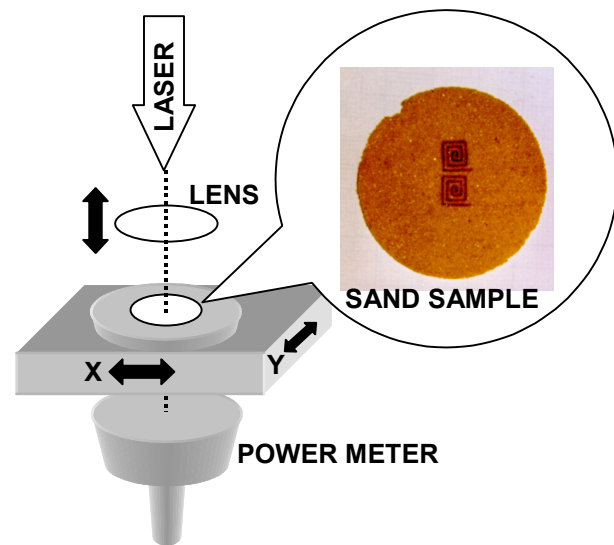


Figure 4. - Experimental configuration for the measurement of the energy transfer

4. Even if the energy released during the heating process (Figure 3.) is four orders of magnitude lower than the laser radiation one, it could be important for the process considering that it is a very localised energy. This phenomenon requires further investigations.
5. The mechanical agglomeration of grains is not included in the thermal modelisation.

Table III - Comparison between experimental results and calculation for Zircon

| Nominal Laser Power | 1 Watt | | 3 Watt | | | | 5 Watt | |
|---------------------|----------------------|--------|----------------------|--------|----------------------|--------|----------------------|--------|
| | $T_{max}[^{\circ}C]$ | p [mm] | $T_{max}[^{\circ}C]$ | p [mm] | $T_{max}[^{\circ}C]$ | p [mm] | $T_{max}[^{\circ}C]$ | p [mm] |
| Spot diameter [mm] | 0.5 | | 0.5 | | 1.2 | | 1.2 | |
| Scan speed [mm/1'] | 490 | | 1290 | | 740 | | 1180 | |
| Experimental | 140 | 0.6 | 174 | 0.5 | 157 | 0.4 | 160 | 0.6 |
| Analytical | 282 | 0.2 | 215 | 0.2 | 245 | 0.8 | 211 | 0.6 |
| Numerical | 370 | 0.3 | 350 | 0.3 | 207 | 0.4 | 277 | 0.4 |

Table IV - Comparison between experimental results and calculation for DB40

| Nominal Laser Power | 1 Watt | | 3 Watt | | | | 5 Watt | |
|---------------------|----------------------|--------|----------------------|--------|----------------------|--------|----------------------|--------|
| | $T_{max}[^{\circ}C]$ | p [mm] | $T_{max}[^{\circ}C]$ | p [mm] | $T_{max}[^{\circ}C]$ | p [mm] | $T_{max}[^{\circ}C]$ | p [mm] |
| Spot diameter [mm] | 0.5 | | 0.5 | | 1.2 | | 1.2 | |
| Scan speed [mm/1'] | 490 | | 1290 | | 740 | | 1180 | |
| Experimental | 162 | 0.8 | 193 | 0.6 | 180 | 0.6 | 200 | 0.6 |
| Analytical | 195 | 0.6 | 153 | 0.2 | 172 | 0.8 | 148 | 0.6 |
| Numerical | 560 | 0.4 | 551 | 0.3 | 327 | 0.5 | 422 | 0.5 |

The discrepancies between the experimental data and the theoretical calculation can be overcome with the following methods:

- a. by introducing corrective parameters determined with specific tests in the interesting range for production purposes;
- b. by changing some basic hypotheses, such as the homogeneous characteristics of the material.

In the last case, this could lead to a very complicated model, making it useless for practical applications.

An alternative approach could be based on an energy balance on a given sand volume between the incident energy and those necessary for the sand heating (calculated by DSC analysis). In this case it would not be necessary to consider the heat conduction problem, in the form of the equations (2) and (6), but the information about the temperature history would be lost. It seems very probable that further improvements in the theoretical calculation will be possible in short time. However it should be emphasised that the main contribution of the methods provided in the present paper comes from the comprehension

of the basic SLS phenomena and not for a strictly quantitative analysis.

ACKNOWLEDGEMENTS

The authors wish to thank Ing. Andrea Pelleriti for his help in the experimental phase, Prof. G. Conti and Prof. G. Levita and A. Marchetti of the Chemical Dept. and the Chemical Eng. Dept. respectively and the personnel of the Mechanical, Nuclear and Production Eng. Dept. of the University of Pisa. Financial support from MURST (60%) is acknowledged.

REFERENCES

- [1] Beaman, J.; Barlow, J.; Bourrel, D.; Crawford, R.; Marcus, H.; McAlea, K.: Solid Freeform Fabrication - A New Direction in Manufacturing, Kluwer Academic Pub., 1997.
- [2] Nelson, J.C.; Vail, N.K.; Barlow, J.; Beaman, J.; Bourrel, D.; Marcus, H.: Selective Laser Sintering of Polymer Coated Silicon Carbide Powders, Ind. Eng. Chem. Res., n. 34 (1995), 1641-1651.
- [3] Papadatos, A.L.; Ahzi, S.; Paul, F.W.: On Enhancing the Selective Laser Sintering Process: Part I: Simulating the Manufacturing Process, Clenson University Report (1995).
- [4] Papadatos, A.L.; Ahzi, S.; Deckard, C.R.; Paul, F.W.: On dimensional stabilities: modelling of the bonus-z during the SLS process, SFF Symp. Proc., Austin Texas (1997).
- [5] Santochi, M.; Tantussi, G.; Dini, G.: Laser Sintering of Pre-Coated Sands using Rapid Prototyping Techniques, 41. Internationales Wissenschaftliches Kolloquium, Band 1, Ilmenau Germany (1996), 387-392.
- [6] CIRP Co-operative Research Working Group on Laser Absorption, Paris, Private Communication (1996)
- [7] Bejan, A.: Heat Transfer, John Wiley and Sons Inc., NY, 1993, 151-154, 182-184.
- [8] Eckert, E.R.G.; Drake, R.M.: Analysis of Heat and Mass Transfer, Mc Graw Hill, New York, 1972, 237-238.
- [9] Patankar, S.: Numerical Heat Transfer and Fluid Flow, McGraw Hill, NY, 1980.
- [10] Show, T. L.; Carrol, J. C.: Application of Baseline Correction to the «Ratio Method» of DSC Specific Heat Determination, 13th Symposium on Thermo-physical Properties, Boulder Colorado (1997).
- [11] Ueda, T.; Yamada, K.; Nakayama, K.: Temperature of Work Materials Irradiated with CO₂ laser, Annals of the CIRP, Vol. 46 (1997) n. 1, 117-122.